



## Structure of states in $^{12}\text{Be}$ via the $^{11}\text{Be}(d, p)$ reaction

R. Kanungo<sup>a,b,\*</sup>, A.T. Gallant<sup>a</sup>, M. Uchida<sup>a</sup>, C. Andreoiu<sup>c</sup>, R.A.E. Austin<sup>a</sup>, D. Bandyopadhyay<sup>a</sup>, G.C. Ball<sup>b</sup>, J.A. Becker<sup>d</sup>, A.J. Boston<sup>e</sup>, H.C. Boston<sup>e</sup>, B.A. Brown<sup>f</sup>, L. Buchmann<sup>b</sup>, S.J. Colosimo<sup>a</sup>, R.M. Clark<sup>g</sup>, D. Cline<sup>h</sup>, D.S. Cross<sup>c</sup>, H. Dare<sup>b</sup>, B. Davids<sup>b</sup>, T.E. Drake<sup>i</sup>, M. Djongolov<sup>b</sup>, P. Finlay<sup>j</sup>, N. Galinski<sup>b,k</sup>, P.E. Garrett<sup>j</sup>, A.B. Garnsworthy<sup>b</sup>, K.L. Green<sup>j</sup>, S. Grist<sup>k</sup>, G. Hackman<sup>b</sup>, L.J. Harkness<sup>e</sup>, A.B. Hayes<sup>h</sup>, D. Howell<sup>b,k</sup>, A.M. Hurst<sup>d</sup>, H.B. Jeppesen<sup>g</sup>, K.G. Leach<sup>j</sup>, A.O. Macchiavelli<sup>g</sup>, D. Oxley<sup>e</sup>, C.J. Pearson<sup>b</sup>, B. Pietras<sup>e</sup>, A.A. Phillips<sup>j</sup>, S.V. Rigby<sup>e</sup>, C. Ruiz<sup>b</sup>, G. Ruprecht<sup>b</sup>, F. Sarazin<sup>l</sup>, M.A. Schumaker<sup>j</sup>, A.C. Shotter<sup>b,m</sup>, C.S. Sumitharachchi<sup>j</sup>, C.E. Svensson<sup>j</sup>, I. Tanihata<sup>n</sup>, S. Triambak<sup>j</sup>, C. Unsworth<sup>e</sup>, S.J. Williams<sup>b</sup>, P. Walden<sup>b</sup>, J. Wong<sup>j</sup>, C.Y. Wu<sup>d</sup>

<sup>a</sup> Astronomy and Physics Department, Saint Mary's University, Halifax, Nova Scotia, B3H 3C3, Canada

<sup>b</sup> TRIUMF, Vancouver, British Columbia, V6T 2A3, Canada

<sup>c</sup> Department of Chemistry, Simon Fraser University, Burnaby, British Columbia, V5A 1S6, Canada

<sup>d</sup> Lawrence Livermore National Laboratory, Livermore, CA 94551, USA

<sup>e</sup> Department of Physics, University of Liverpool, Liverpool, L69 7ZE, United Kingdom

<sup>f</sup> Department of Physics and Astronomy, Michigan State University, East Lansing, MI 48824, USA

<sup>g</sup> Nuclear Science Division, Lawrence Berkeley National Laboratory, Berkeley, CA 94720, USA

<sup>h</sup> Department of Physics and Astronomy, University of Rochester, Rochester, NY 14627, USA

<sup>i</sup> Department of Physics, University of Toronto, Toronto, Ontario, M5S 1A7, Canada

<sup>j</sup> Department of Physics, University of Guelph, Guelph, Ontario, N1G 2W1, Canada

<sup>k</sup> Department of Physics, Simon Fraser University, Burnaby, British Columbia, V5A 1S6, Canada

<sup>l</sup> Physics Department, Colorado School of Mines, Golden, CO 80401, USA

<sup>m</sup> Department of Physics and Astronomy, University of Edinburgh, Edinburgh, United Kingdom

<sup>n</sup> Research Center for Nuclear Physics, Osaka University, Mihogaoka, Ibaraki, Osaka 567 0047, Japan

### ARTICLE INFO

#### Article history:

Received 12 August 2009

Received in revised form 10 November 2009

Accepted 10 November 2009

Available online 14 November 2009

Editor: D.F. Geesaman

#### PACS:

21.10.Gv

21.10.Jx

21.10.Pc

21.60.Cs

24.10.Eq

25.60.Je

27.10.+h

#### Keywords:

Transfer reactions

Inverse kinematics

Radioactive beams

Shell structure

### ABSTRACT

The *s*-wave neutron fraction of the  $0^+$  levels in  $^{12}\text{Be}$  has been investigated for the first time through the  $^{11}\text{Be}(d, p)$  transfer reaction using a 5 A MeV  $^{11}\text{Be}$  beam at TRIUMF, Canada. The reaction populated all the known bound states of  $^{12}\text{Be}$ . The ground state *s*-wave spectroscopic factor was determined to be  $0.28^{+0.03}_{-0.07}$  while that for the long-lived  $0_2^+$  excited state was  $0.73^{+0.27}_{-0.40}$ . This observation, together with the smaller effective separation energy indicates enhanced probability for an extended density tail beyond the  $^{10}\text{Be}$  core for the  $0_2^+$  excited state compared to the ground state.

© 2009 Elsevier B.V. Open access under CC BY license.

\* Corresponding author at: Astronomy and Physics Department, Saint Mary's University, Halifax, Nova Scotia B3H 3C3, Canada.

E-mail address: ritu@triumf.ca (R. Kanungo).

0370-2693 © 2009 Elsevier B.V. Open access under CC BY license.

doi:10.1016/j.physletb.2009.11.025

Understanding the structure evolution from stable to halo nuclei requires systematic studies of changes in orbital occupancies. So far only Borromean nuclei, with unbound core + *n* clusters, have

shown a two-neutron halo structure, such as in  $^{11}\text{Li}$  [1]. The existence of such a structure in a non-Borromean nucleus is not yet established and investigating this in  $^{12}\text{Be}$  is of particular interest. The disappearance of the conventional  $N = 8$  magic number in  $^{12}\text{Be}$  is suggested from the lowering of the  $2_1^+$  state [2]. This is associated with the  $2s_{1/2}$  and  $1d_{5/2}$  orbitals intruding into the  $p$ -shell.  $^{11}\text{Be}$  is known to be a one-neutron halo with the neutron dominantly occupying the  $2s_{1/2}$  orbital with spectroscopic factor  $S \sim 0.74$  in agreement with the one-neutron removal cross-section [3]. This is also in agreement with the observations from transfer reactions [4–6].

The one-neutron separation energy ( $S_n$ ) of  $^{12}\text{Be}$  is 3169(16) keV, while that of  $^{11}\text{Be}$  is 504(6) keV [7], and  $^{11}\text{Li}$  has a two-neutron separation energy of 369.15(65) keV [8]. An important question is how the increase in neutron separation energy due to pairing influences the neutron distribution in the  $2s_{1/2}$  orbital.

Here we report the first measurement that determines the  $s$ -wave neutron occupancy of the  $0^+$  bound states in  $^{12}\text{Be}$  through the  $^{11}\text{Be}(d, p)^{12}\text{Be}$  neutron-transfer reaction. Since the ground state of  $^{11}\text{Be}$  is  $1/2^+$ , the selectivity of this reaction offers a clean way to disentangle the  $s$ -wave occupancies for the  $0^+$  levels. The results are therefore the first clean determination of the  $^{12}\text{Be}_{\text{gs}}$  spectroscopic factor without any influence of the isomeric  $0^+$  excited state. The observations also show the  $s$ -wave composition of the  $0^+$  excited state.

The first excited state ( $2^+$ ) in  $^{12}\text{Be}$  was observed at 2.11(2) MeV through inelastic scattering [2,9] and heavy ion transfer [10]. A state at 2.68(3) MeV, was interpreted as an  $l = 1$  excitation [9, 12] which is considered to be the same state as observed in the  $^{10}\text{Be}(t, p)^{12}\text{Be}$  reaction at 2.73(3) MeV [11]. Recently, a long-lived  $0^+$  state at 2.24(2) MeV [13] was populated in the production of a  $^{12}\text{Be}$  secondary beam. The mean lifetime of the state was determined to be 331(12) ns [14]. The presence of this state makes it important to investigate the  $s$ -wave configuration in the two bound  $0^+$  levels of  $^{12}\text{Be}$ .

The spectroscopic factor ( $S$ ) for the  $^{11}\text{Be}_{\text{gs}} + n(2s_{1/2})$  configuration in  $^{12}\text{Be}_{\text{gs}}$  was found to be  $0.42 \pm 0.06$  from a one-neutron removal reaction [15]. This is smaller than the  $2s_{1/2}$  component in  $^{11}\text{Be}$  as expected due to larger neutron separation energy. The  $^{12}\text{Be}_{\text{gs}}$  has  $p$ -wave and  $d$ -wave spectroscopic factors of  $0.37 \pm 0.06$  [15] and  $0.48 \pm 0.06$  [16], respectively. The small  $s$ -wave probability in  $^{12}\text{Be}$  makes it necessary to explore whether any of the bound excited levels have a  $^{11}\text{Be}_{\text{gs}} + n(2s_{1/2})$  configuration. It should be mentioned here that in the neutron removal reactions the  $^{12}\text{Be}$  beam cannot be distinguished as being in its ground state or its  $0_2^+$  long-lived state. It is therefore of utmost importance to find the  $s$ -wave strength through a different method that is free from this problem. In this work, the  $^{11}\text{Be}(d, p)^{12}\text{Be}$  reaction provides the first clean signature of the  $s$ -wave strength for the ground state and the  $0_2^+$  state.

Theoretically, the  $s$ -wave spectroscopic factor for the  $0_2^+$  level was predicted in [17] to be 1.34, but it is stated that these numbers should not be taken too seriously, since the matrix elements used are appropriate to a  $^{12}\text{C}$  core. Ref. [18], with different wavefunctions, discusses an increased  $s$ -wave spectroscopic factor of 1.06 for the ground state while that for the excited  $0_2^+$  state is predicted to be 0.54.<sup>1</sup> Models of  $^{11,12}\text{Be}$  based on a deformed potential [19] consider the ground state and the  $0_2^+$  excited state to be linear combinations of  $1/2[220]^2$  and  $1/2[101]^2$  two-neutron configurations with equal amplitudes. A study based on a  $^{10}\text{Be} + n + n$

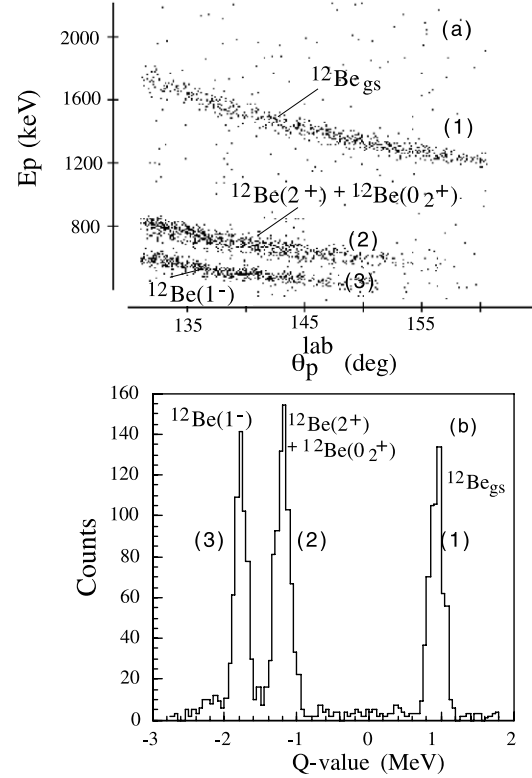


**Fig. 1.** (a) The kinematic loci of the protons identified in the upstream silicon detector in coincidence with  $^{12}\text{Be}$  in the downstream silicon detector. (b) The  $Q$ -value spectrum integrated over the full angular range. The different states of  $^{12}\text{Be}$  are labeled in the figure.

three-body structure model discussed the second  $0^+$  excited state to have two neutrons in the  $1p_{1/2}$  orbital [20]. No experimental information exists on the detailed configuration of the excited states in  $^{12}\text{Be}$ .

The experiment was performed at the ISAC-II facility, TRIUMF, Canada. The radioactive  $^{11}\text{Be}$  beam was extracted from the TRILIS laser ion source [21], and accelerated to 5 A MeV by the ISAC-I room-temperature RFQ and DTL [22] accelerators, followed by the new ISAC-II superconducting linear accelerator. The uncertainty in the average beam energy was  $< 10$  A keV. An accelerated beam intensity of typically  $10^5$  ions/s was delivered to a  $40 \mu\text{g}/\text{cm}^2$  self supporting  $(\text{CD}_2)_n$  reaction target whose thickness was measured from energy-loss using a standard alpha source. The beam spot size at the target was  $< 3$  mm in diameter.

A  $140 \mu\text{m}$  thick annular S3 type double-sided silicon strip detector detected the protons in the backward direction covering laboratory angles of  $130^\circ$ – $160^\circ$ . The 24 ring segments of the detector defined the scattering angle. The reverse side of the detector is segmented azimuthally into 32 sectors. The scattered  $^{12}\text{Be}$  along with  $^{11}\text{Be}$  from elastic scattering were detected in another annular silicon detector placed 75 cm downstream of the reaction target with laboratory angular coverage of  $0.8^\circ$ – $2.7^\circ$ . This coverage ensured detection of the protons and  $^{12}\text{Be}$  nuclei in coincidence. The coincident detection suppressed nearly all the background events making it possible to identify the kinematic loci for the  $^{11}\text{Be}(d, p)^{12}\text{Be}$  reaction through proton energy and angle correlations (Fig. 1a). The coincidence efficiency was determined from a Monte Carlo simulation and the region with efficiency  $\geq 70\%$  is shown in Fig. 3.

The  $Q$ -value spectrum constructed from the energy and angle of the detected protons is shown in Fig. 1b integrated over the

<sup>1</sup> This value is considering the  $s^2$  wavefunction probability to be 0.27 instead of 0.17 which is likely a misprint in [18] because it does not lead to a total probability of unity.

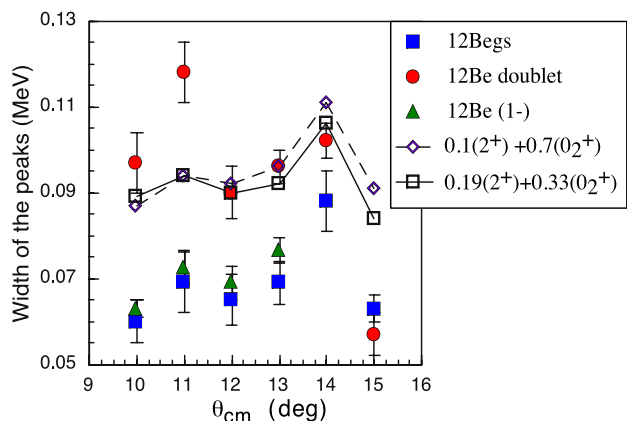


**Fig. 2.** Gaussian width ( $\sigma$ ) of the Q-value peaks for  $^{12}\text{Be}_{gs}$  (filled squares),  $^{12}\text{Be}(2^+ + 0_2^+)$  (filled circles) and  $^{12}\text{Be}(1^-)$  (filled triangles) states for different center-of-mass angles. The dashed-line connecting the open diamonds shows the simulated width for a mixture of  $0.10(2^+) + 0.73(0_2^+)$ . The solid line connecting the open squares shows the simulated width for  $0.19(2^+) + 0.33(0_2^+)$ .

full angular range. The kinematic curves and Q-value peaks labeled as (1), (2), (3) in Figs. 1a and 1b correspond to the  $^{12}\text{Be}_{gs}$ , a doublet consisting of the  $2^+$  and  $0_2^+$  excited states and the  $1^-$  excited state respectively. The Q-value resolution on an average was around 65 keV ( $\sigma$ ) observed for the  $^{12}\text{Be}_{gs}$  peak at a fixed  $\theta_{cm}$  bin. The detailed resolution for each angle bin is shown in Fig. 2.

The width ( $\sigma$ ) of the Q-value peak, for the different states obtained from a single Gaussian fit to each peak is shown in Fig. 2. The centroid, width and amplitude of the Gaussian were free parameters in the fit. The widths of the  $^{12}\text{Be}_{gs}$  and the  $1^-$  state are found to be similar to each other. However, the second Q-value peak (2) is much wider than the ground state peak for  $\theta_{cm} = 10^\circ$ – $13^\circ$ , indicating that this peak is a mixture of two states. The different distribution of the widths over angles from that of other states, suggests the admixture of different angular momentum transitions. This clearly shows that the second peak (2) is not a pure  $2^+$  state or a pure  $0_2^+$  state. The statistical uncertainties shown in Fig. 2 are larger for  $\theta_{cm} = 10^\circ$  and  $11^\circ$  because of smaller statistics due to lower coincidence efficiency. The peak at  $\theta_{cm} = 15^\circ$  is at the limit of detection in excitation energy and therefore has a lower efficiency for the higher excitation energy (i.e. smaller Q-value) direction of the peak, which probably leads to its smaller observed width. We clarify here that the Q-value peaks shown in Fig. 1b are angle integrated and their widths contain combined effects of varying resolutions for different strips in the detector and small shifts in centroids with angles. The maximum shift in centroid is  $\sim 50$  keV. Therefore, the overall width of the peak (2) in Fig. 1b though slightly larger than the ground state is not an accurate way to view the presence of a doublet; rather the presence is more clearly indicated in the peaks widths of individual angle spectra shown in Fig. 2. The simulated open diamond points (Fig. 2) are shown with the spectroscopic factors for the best fit to the angular distribution in Fig. 3b ( $0.10(2^+) + 0.73(0_2^+)$ ). The open square points (Fig. 2) use the spectroscopic factor from the upper-error bar for ( $2^+$ ) and lower-error bar for ( $0_2^+$ ) obtained from the chisquare fit to the angular distribution in Fig. 3b.

The intensity of the  $^{11}\text{Be}$  beam was determined in two ways throughout the experiment. The beam passing through the hole in the annular silicon detector was stopped and counted using a  $30\text{ mm} \times 30\text{ mm}$  YAP:Ce radiation hard inorganic scintillator. In addition, the Rutherford scattering from carbon in the target provided an independent measure of the beam intensity. The two methods were in agreement which adds further support to the target thickness being used in the experiment. The deuteron component in

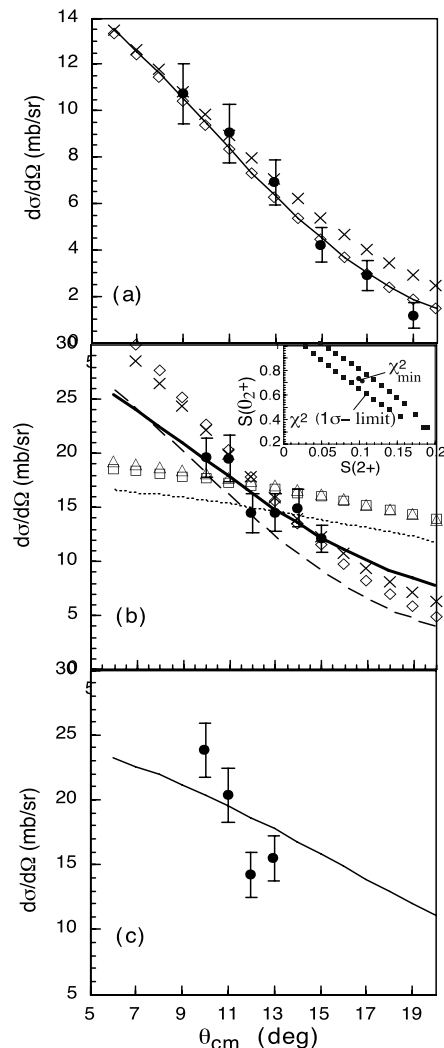


**Fig. 3.** (a) The angular distribution data for  $^{12}\text{Be}_{gs}$ , Q-value peak (1). The diamonds (cross marks) represent the DWBA calculation with  $S = 0.23$  for a neutron in the  $2s_{1/2}$  orbital using potential Set1 (Set2) and a Woods-Saxon form factor. The solid line is that with  $S = 0.28$  using a Reid soft core form factor. (b) The combined angular distribution for the  $^{12}\text{Be}(2^+)$  and  $^{12}\text{Be}(0_2^+)$  states Q-value peak (2). The solid line is the best fit with  $s$ -wave ( $S = 0.73$ ) +  $d$ -wave ( $S = 0.10$ ) with potential Set1 and Reid soft core form factor. With the same form factor, the dashed and dotted lines are  $s$ -wave ( $S = 1$ ) and  $d$ -wave ( $S = 0.25$ ) respectively. Using the Woods-Saxon form factor, the  $d$ -wave ( $S = 0.25$ ) is shown by triangles (squares) and the  $s$ -wave ( $S = 1$ ) is shown by diamonds (cross marks) for potential Set1 (Set2). The inset shows the chisquare minimum and the joint 68% confidence level region. (c) Angular distribution of the  $1^-$  state Q-value peak (3) compared to a DWBA calculation (Set1) with spectroscopic factor 0.35.

the target relative to carbon is fixed by the chemical composition of the  $(\text{CD}_2)_n$  material. The uncertainty in the beam intensity was considered to be 5%.

The differential cross-section as a function of center of mass scattering angle (Fig. 3) was obtained by selecting the respective Q-value peak. The small background under the peak was estimated using a linear shape for the background and a Gaussian shape for the peak. The error bars shown in Fig. 3 are the statistical errors. The systematic error includes an overall 10% uncertainty due to the target thickness, and angle dependent uncertainties due to the coincidence efficiency that range from 1%–10%.

Obedying the selection rules, the  $^{11}\text{Be}(d, p)$  reaction can populate the  $0^+$  states in  $^{12}\text{Be}$  only if the transferred neutron occupies the  $2s_{1/2}$  orbital. The population of the  $2^+$  and  $1^-$  states are pos-

**Table 1**  
Optical potential parameters used.

Channel	$V_0$ (MeV)	$r_0$ (fm)	$a_0$ (fm)	$W_v$ (MeV)	$W_d$ (MeV)	$r_l$ (fm)	$a_l$ (fm)	$V_{so}$ (MeV)	$r_{so}$ (fm)	$a_{so}$ (fm)
$d(\text{Set1})$	80.53	1.17	0.80	5.19	4.71	1.56	0.80	3.54	1.23	0.81
$d(\text{Set2})$	118.0	0.87	0.91	0.00	5.80	1.57	0.78	5.80	0.87	0.91
$p(\text{Set1})$	58.59	1.12	0.67	0.85	5.26	1.3	0.51	5.53	0.90	0.59
$p(\text{Set2})$	57.8	1.25	0.25	0.00	8.08	1.4	0.22	6.5	1.25	0.25

sible with the transferred neutron occupying the  $1d_{5/2}$  and  $1p_{1/2}$  orbitals, respectively.

To extract the spectroscopic strength the experimental angular distributions were compared to finite range distorted wave Born approximation (DWBA) calculations using the code DWUCK5 [23]. The entrance and exit channel optical potentials were based on global parametrizations (Set1) of deuteron–nucleus [24] and proton–nucleus [25] interactions. The interactions were of the Woods–Saxon form [23]

$$V(r) = -V_0 f(x_0) - i \left( W_v f(x_l) - 4W_d \frac{df(x_l)}{dx_l} \right) + V_{so} \left( \frac{\hbar}{m_\pi c} \right)^2 \frac{1}{r} \frac{df(x_{so})}{dr} (\vec{L} \cdot \vec{s})$$

where

$$f(x_i) = 1/[1 + \exp(x_i)], \quad x_i = (r - r_i A^{1/3})/a_i, \quad i = 0, l, so.$$

Calculations using potential parameters (Set2) from  $^{10}\text{Be} + d$  [4] and  $^{12}\text{C} + p$  [26] are close to the results obtained with Set1 in our region of interest (Fig. 3). The parameters are listed in Table 1.  $V_{so}^D = -4V_{so}$  MeV fm<sup>2</sup> is used for DWUCK. The bound-state potential for  $^{11}\text{Be} - n$  was of Woods–Saxon form where the depth of the potential was adjusted to reproduce the effective separation energies ( $S_n^{\text{eff}} = S_n - E^*(^{12}\text{Be})$ ) for each state. For the  $p-n$  potential we investigated using both the microscopic Reid soft core potential and the Woods–Saxon form. The uncertainty in the spectroscopic factors includes the result from both these types of  $p-n$  form factors. The experimental spectroscopic factors ( $S$ ) for the  $^{12}\text{Be}$  states are obtained through the relation

$$\left( \frac{d\sigma}{d\Omega} \right)_{\text{exp}} = S_d \frac{(2J_f + 1)}{(2J_i + 1)} S \left( \frac{d\sigma}{d\Omega} \right)_{\text{DWUCK}}$$

where  $S_d$  is considered to be 1.0 [23].  $J_i$  and  $J_f$  are the spins of the initial and final nuclei.

The solid line in Fig. 3a shows the DWBA result for the  $^{12}\text{Be}_{\text{gs}}$ . The  $s$ -wave parentage extracted from a  $\chi^2$  minimization with both statistical and systematic errors is  $S = 0.28_{-0.07}^{+0.03}$  in the 68% confidence level ( $\chi_{\text{min}}^2 + 1$ ). This is reduced compared to  $^{11}\text{Be}$  showing the effect of pairing. This spectroscopic factor derived from the  $^{11}\text{Be}(d, p)$  reaction is free from any influence of the  $0_2^+$  state. The present result is therefore an important finding that can provide some guidance to the theoretical models.

Fig. 3b shows the angular distribution that is the sum of  $^{12}\text{Be}$  in its  $2^+$  and  $0_2^+$  states. The dotted curve is the DWBA prediction for the  $^{12}\text{Be}(2^+)$  with the neutron in the  $d_{5/2}$  orbital and a spectroscopic factor of 0.25. The dashed curve shows the result for the  $^{12}\text{Be}(0_2^+)$  excited state with the neutron in the  $2s_{1/2}$  orbital with  $S = 1$ . The data are then fitted with  $S1 \cdot (^{11}\text{Be} \times n(1d_{5/2})) + S2 \cdot (^{11}\text{Be} \times n(2s_{1/2}))$ , where  $S1$  and  $S2$  are the spectroscopic factors for the  $d$ -wave and  $s$ -wave neutron in the  $2^+$  and  $0_2^+$  states in  $^{12}\text{Be}$  respectively. The best fit (solid line) with a joint 68% confidence level uncertainty ( $\chi_{\text{min}}^2 + 2.3$ ) results in  $s$ -wave strength

of  $S2 = 0.73_{-0.40}^{+0.27}$  for the  $0_2^+$  state, while the  $d$ -wave strength is found to be  $S1 = 0.10_{-0.07}^{+0.09}$  for the  $2^+$  state weighted by the statistical uncertainties. The uncertainties considering  $\chi_{\text{min}}^2 + 1$  results in  $S1 = 0.10_{-0.05}^{+0.06}$  and  $S2 = 0.73_{-0.26}^{+0.25}$ . The 2 sigma limit of the joint probability could theoretically suggest a pure  $2^+$  contribution with  $S1 = 0.25$  to the angular distribution. However, the width of the  $Q$ -value peaks show the  $2^+ - 0_2^+$  doublet nature suggesting contrary to this. Further experiments towards a more precise determination of the parentage for the  $2^+$  and  $0_2^+$  states might be undertaken in the future.

The  $s$ -wave component of the two-neutron density for the  $0_2^+$  state with the spectroscopic factor of 0.73–0.33, has the probability of 60%–27% of being found outside the  $^{10}\text{Be}$  core radius of 3.3 fm, which is the point within which 90% of the core probability density is found. In comparison, the fraction of the  $s$ -wave component of the two-neutron density in the  $^{12}\text{Be}_{\text{gs}}$  outside the core is only 14%–20% for a spectroscopic factor of 0.21–0.31. This radial extent supports the indication of a halo-like structure in the  $0_2^+$  state. Further experimental and theoretical investigations to understand this in more details will be useful in future.

The normalization to the data shows an approximate spectroscopic factor of  $\sim 0.35$  for the state at 2.68 MeV (Fig. 3c). This state being close to the threshold of detection we do not assign confidence bands. One cannot rule out the possibility of population of a higher  $0^+$  state though, the shell model predictions suggest such a state to be located at much higher excitation energy. This cannot be confirmed at present since the level is close to the detection threshold. The nearly similar magnitudes of the cross-sections for the different states in  $^{12}\text{Be}$  provides additional signature for the presence of intruder orbitals in them as confirmed through the  $s$ -wave component of the states this experiment.

Energies and spectroscopic factors were calculated in the  $s$ - $p$ - $sd$ - $pf$  model space with the WBP Hamiltonian [27], which was designed for configurations confined to a fixed number of harmonic oscillator excitations. In this limit the  $^{11}\text{Be}$  ground state has a  $1\hbar\omega$  configuration, and states in  $^{12}\text{Be}$  have  $N\hbar\omega$  with  $N = 0$  for the pure  $p$ -shell configuration. The lowest  $N = 0$  and  $N = 2$   $0^+$  configurations are nearly degenerate and have spectroscopic factors of 0 and 0.89, respectively. The mixing between  $N = 0, 2$  and  $N = 1, 3$  configurations can be done with an additional gap-energy parameter ( $\Delta_{psd}$ ) [28]. We choose  $\Delta_{psd} = -1.85$  MeV to give a ground state which is 32%  $N = 0$  and 68%  $N = 2$  (*shell1* in Table 2) that was deduced from the  $^{12}\text{Be}$  knockout experiment [15]. The resulting spectroscopic factors are given in Table 2 ( $S^{\text{shell1}}$ ). The WBP results should be regarded as an extrapolation from the (large) set of data (mostly for nuclei near stability) used to determine the WBP Hamiltonian [27]. We can expect uncertainties related to the gap-energy parameter as well as changes in the Hamiltonian for these nuclei being near the neutron drip line. A  $^{12}\text{Be}$  ground state with 50%  $N = 0$  and 50%  $N = 2$  (*shell2* in Table 2) reduces the  $s$ -wave spectroscopic factor for the ground state. Reducing the energy gap to  $-1.2$  MeV and lowering the  $1d_{5/2}$  orbital by 0.8 MeV with a ground state of 42%  $N = 0$  and 58%  $N = 2$  (*shell3* in Table 2) we get a reduced spectroscopic factor for the  $2^+$  state and the ground state.

**Table 2**

Energies and spectroscopic factors with WBP for the mixed  $N = 0$  and  $2$  and  $N = 1$  and  $3$  configurations. The uncertainties for the excited  $0^+$  and  $2^+$  states originate from the statistical error bars in Fig. 3b.

$J$	$(l)$	$E_x^{shell1}$ (MeV)	$S^{shell1}$	$E_x^{shell2}$ (MeV)	$S^{shell2}$	$E_x^{shell3}$ (MeV)	$S^{shell3}$	$E_{exp}$ (MeV)	$S_{exp}$
$0^+$	(s)	0.00	0.57	0.00	0.39	0.00	0.29	0.00	$0.28^{+0.03}_{-0.07}$
$0^+$	(s)	1.71	0.55	1.65	0.72	1.82	0.45	2.24(2) [13]	$0.73^{+0.27}_{-0.40}$
$2^+$	(d)	2.36	0.50	2.59	0.55	2.46	0.41	2.11(2) [2]	$0.10^{+0.09}_{-0.07}$
$1^-$	(p)	3.71	0.55	3.38	0.56	3.38	0.52	2.68(3) [12]	( $\sim 0.35$ )
$0^-$	(p)	5.91	0.57	5.59	0.62	5.60	0.40	–	–
$0^+$	(s)	5.53	0.82	5.79	0.83	5.81	0.86	–	–

We mention here that the theoretical calculations presented in this Letter are only a first attempt to interpret the data. Further theoretical calculations would certainly be useful but these are beyond the scope of this Letter.

In summary, the first determination of the  $s$ -wave strength in  $^{12}\text{Be}$  through the  $^{11}\text{Be}(d, p)$  one-neutron transfer reaction at 5 A MeV is reported. Since the ground state of  $^{11}\text{Be}$  has a spin of  $1/2^+$  this reaction is selective to the  $s$ -wave neutron component in the  $0^+$  levels. The nucleus  $^{12}\text{Be}$  was populated in its ground state as well as the bound excited states. This experiment is the first clean extraction of  $^{12}\text{Be}_{gs}$   $s$ -wave spectroscopic factor free from any influence of the  $0_2^+$  long-lived state. The ground state of  $^{12}\text{Be}$  was found to have an  $s$ -wave spectroscopic factor of  $0.28^{+0.03}_{-0.07}$  while the excited  $0^+$  level shows an  $s$ -wave spectroscopic factor of  $0.73^{+0.27}_{-0.40}$ . This result, together with the small effective neutron separation energy ( $S_n^{eff} \sim 930$  keV) for the  $0_2^+$  state provides some indication that the long-lived  $0_2^+$  state in  $^{12}\text{Be}$  may have a neutron halo-like structure. These observations are an important step to reveal the change of  $s$ -wave strength as an effect of pairing.

### Acknowledgements

The authors thank the TRIUMF accelerator staff and the ISAC beam delivery group. Thanks are due to the laser ionization group led by J. Lassen for monitoring the  $^{11}\text{Be}$  beam production. The authors gratefully acknowledge NSERC for supporting this work. TRIUMF receives federal funding via a contribution agreement with the National Research Council, Canada. Sincere thanks are due to P. Morrall of Daresbury National Laboratory for preparing the  $(\text{CD}_2)_n$  target. The work at LLNL is supported by DOE under con-

tract DE-AC52-07NA27344, that at LBNL is supported in part by DOE under contract No. DE-AC02-05CH11231 and that at University of Rochester is supported by NSF. This work is supported in part by NSF grant PHY-0758099. Discussions with P.D. Kunz are gratefully acknowledged.

### References

- [1] I. Tanihata, et al., Phys. Rev. Lett. 55 (1985) 2676.
- [2] H. Iwasaki, et al., Phys. Lett. B 481 (2000) 7.
- [3] T. Aumann, et al., Phys. Rev. Lett. 84 (2000) 35.
- [4] D.L. Auton, et al., Nucl. Phys. A 157 (1970) 305.
- [5] B. Zwieglinski, et al., Nucl. Phys. A 315 (1979) 124.
- [6] S. Fortier, et al., Phys. Lett. B 461 (1999) 22.
- [7] G. Audi, et al., Nucl. Phys. A 729 (2003) 337.
- [8] M. Smith, et al., Phys. Rev. Lett. 101 (2008) 202501.
- [9] H. Iwasaki, et al., Phys. Lett. B 491 (2000) 8.
- [10] G.C. Ball, et al., Phys. Lett. B 49 (1974) 33.
- [11] H.T. Fortune, et al., Phys. Rev. C 50 (1994) 1355.
- [12] S. Shimoura, et al., Nucl. Phys. A 738 (2004) 162.
- [13] S. Shimoura, et al., Phys. Lett. B 560 (2003) 31.
- [14] S. Shimoura, et al., Phys. Lett. B 654 (2007) 87.
- [15] A. Navin, et al., Phys. Rev. Lett. 85 (2000) 266.
- [16] S.D. Pain, et al., Phys. Rev. Lett. 96 (2006) 032502.
- [17] F.C. Barker, J. Phys. G 2 (1976) L45.
- [18] H.T. Fortune, R. Sherr, Phys. Rev. C 74 (2006) 024301.
- [19] I. Hamamoto, S. Shimoura, J. Phys. G 34 (2007) 2715.
- [20] C. Romero-Redondo, et al., Phys. Rev. C 77 (2008) 054313.
- [21] E.J. Prime, et al., Hyperfine Int. 171 (2006) 127.
- [22] R.E. Laxdal, Nucl. Instrum. Methods B 204 (2003) 400.
- [23] P.D. Kunz, <http://spot.colorado.edu/~kunz/DWBA.html>.
- [24] Y. Han, et al., Phys. Rev. C 74 (2006) 044615.
- [25] A.J. Koning, J.P. Delaroche, Nucl. Phys. A 713 (2003) 231.
- [26] J.R. Comfort, B.C. Karp, Phys. Rev. C 21 (1980) 2162.
- [27] E.K. Warburton, B.A. Brown, Phys. Rev. C 46 (1992) 923.
- [28] E.K. Warburton, et al., Phys. Lett. B 293 (1992) 7.